Published in final edited form as:

FASEB J. 2020 November ; 34(11): 14946–14959. doi:10.1096/fj.202001234R.

Rspo1/Rspo3-LGR4 signaling inhibits hepatic cholesterol synthesis through AMPKα-SREBP2 pathway

Shiying Liu[1,△], **Yuan Gao**[1,△], **Liping Zhang**[2], **Yue Yin**[1,*], **Weizhen Zhang**[1,2,*]

[1.]School of Basic Medical Sciences, Peking University, Beijing 100191, China

[2.]Department of Surgery, University of Michigan Medical Center, Ann Arbor, MI 48109-0346, USA

Abstract

R-spondins (Rspos) are endogenous ligands of leucine-rich repeat-containing G-protein coupled receptor 4 (LGR4). Rspos-LGR4 signaling plays important roles in embryogenesis, gastrointestinal homeostasis and food intake. Here, we investigated impacts of Rspos-LGR4 on hepatic cholesterol synthesis. Rspo1/3 and *Lgr4* knockdown mice were used to investigate the impacts of Rspo1/3-LGR4 on hepatic cholesterol synthesis. AMPKα agonist, antagonist and shRNA were used to explore the downstream targets of Rspos-LGR4 signaling. In our study, we reported that LGR4, Rspo1 and Rspo3 were highly expressed in hepatocytes and their expressions were sensitive to energy states. Rspo1 and Rspo3 reversed OA-induced cholesterol synthesis, accompanying with increased phosphorylation of AMPKα Thr172, reduced SREBP2 nuclear translocation and *Srebf2* mRNA expression. Conversely, hepatic LGR4 knockdown increased hepatic cholesterol synthesis and decreased phosphorylation of AMPKα both *in vitro* and *in vivo*. Activation or inhibition of AMPKα significantly abolished the effects of LGR4 deficiency or Rspos, respectively, on cholesterol synthesis. Knockdown of AMPKα1 or/and AMPKα2 repressed Rspos induced inhibition on cholesterol synthesis. Our study indicates that Rspo1/Rspo3-LGR4 signaling in hepatocytes suppresses cholesterol synthesis via AMPKα-SREBP2 pathway.

Keywords

Liver; R-spondins; LGR4; AMPK; Cholesterol

1. Introduction

Non-alcoholic fatty liver disease (NAFLD) is a set of metabolic disorders characterized by increased hepatic lipid deposit, including non-alcoholic fatty liver (NAFL), non-alcoholic steatohepatitis (NASH) and liver cirrhosis. NAFLD has become one of the most common

[*]**Correspondence:** Weizhen Zhang, Department of Physiology and Pathophysiology, School of Basic Medical Sciences, Peking University Health Science Center, Beijing 100191, China, weizhenzhang@bjmu.edu.cn; Tel: 0086-10-82802183 or Yue Yin, Department of Physiology and Pathophysiology, School of Basic Medical Sciences, Peking University Health Science Center, Beijing 100191, China, yueyin@bjmu.edu.cn; Tel: 0086-10-82802514.

[△]Shiying Liu and Yuan Gao should be considered joint first author.

6. Author Contributions

Shiying Liu, Yue Yin and Weizhen Zhang designed research; Shiying Liu, Yuan Gao and Liping Zhang performed research; Shiying Liu and Yuan Gao analyzed data; Shiying Liu drafted the paper; Shiying Liu, Yue Yin and Weizhen Zhang revised the paper.

chronic liver diseases worldwide (1). Despite of considerable efforts in the study of NAFLD, its effective intervention remains limited. Researches have validated that the progression of NAFLD is accompanied with elevated cholesterol content in liver. In particular, the severity of NAFLD is positively correlated with increased hepatic synthesis of cholesterol (2). A lipidomic analysis of NAFLD also revealed a stepwise increment of hepatic free cholesterol in NASH compared with NAFL (3). Consistently, clinical studies suggested that pharmaceutical interventions of cholesterol synthesis or absorption significantly alleviate inflammation and fibrosis of NAFLD patients (4, 5). All these findings indicated that intervention of cholesterol synthesis may also benefit the control of NAFLD, in addition to atherosclerosis.

The maintenance of hepatic cholesterol homeostasis depends on the balance between cholesterol synthesis and removal. Previous studies revealed that both extracellular signals and intracellular molecules contribute to the dynamic control of hepatic cholesterol metabolism (6). One of the key intracellular modulators is sterol regulatory element binding protein 2 (SREBP2) (6). Encoded by *Srebf2* gene, SREBP2 precursor is anchored on endoplasmic reticulum (ER) membrane and forms a heterodimeric complex with another ER membrane-bound protein—SREBP cleavage activation protein (SCAP) (7). In response to sterol depletion, SREBP2-SCAP complex on ER membrane dissociates with ER-resident protein—insulin induced gene (Insig), and transports from ER membrane to Golgi where Golgi-localized Site-1 protease (S1P) and Site-2 protease (S2P) release the SREBP2 N terminus (SREBP2-N) from the membrane via proteolysis. Subsequently, SREBP2-N translocates into nucleus to interact with sterol regulatory element (SRE) of target genes to induce transcription of relevant genes, leading to the increase of cholesterol synthesis (8).

Leucine-rich repeat G-protein-coupled receptor 4 (LGR4), a member of subtype B of LGRs, is broadly expressed in cartilage, heart, hair follicle and liver in mammals (9, 10). Its endogenous ligands have been identified to be R-spondins (Rspos), which compose of Rspo1~Rspo4. Rspos-LGR4 signaling plays a pivotal role during embryogenesis as *Lgr4* null mice demonstrate severe intrauterine growth retardation and perinatal death (11). Additionally, Rspos-LGR4 signaling is involved in multiple physiological and pathophysiological processes, such as gastrointestinal homeostasis, tumorigenesis and food intake (12, 13). Of note, several recent studies have shed light on probable functions of Rspos-LGR4 axis in lipid metabolism. In skeletal muscle, *Lgr4* homozygous mutation exhibited promoted lipid oxidation under fasting condition (14). Another study uncovers that *Lgr4* deficient mice are resistant to diet- or genetic-induced obesity due to the promotion of white-to-brown fat switch (15). Moreover, the expression pattern of *Lgr4* in liver exhibits a circadian rhythm. *Lgr4* homozygous mutant mice display dampened circadian rhythms of plasma triglyceride (16). Whether Rspos-LGR4 signaling alters cholesterol metabolism remains unexplored. The present study focuses on clarifying the impact of Rspos-LGR4 signaling on hepatic cholesterol metabolism and its underlying mechanism.

2. Material and Methods

2.1. Materials

Compound C, oleic acid (OA), palmitic acid (PA) and collagenase IV were purchased from Sigma Aldrich (St. Louis, MO, USA). AICAR was purchased from MCE (NJ, USA). R-spondin1 and R-spondin3 were purchased from R&D system (Minneapolis, MN). Rabbit anti-LGR4 was from Santa Cruz Biotechnology (Santa Cruz, CA). Rabbit anti-AMPKα, rabbit anti-pAMPKα (Thr 172) and rabbit anti-β-catenin were obtained from Cell Signaling Technology (Beverly, MA). Rabbit anti-SREBP2, rabbit anti-AMPKα1, rabbit anti-AMPKα2 were from Abcam (Cambridge, MA). Mouse anti-β-actin and mouse anti-laminB1 were purchased from Proteintech (Chicago, USA). RNAtrip was obtained from Applygen (Beijing, China). Reverse transcription (RT) system was from Invitrogen Inc. (Carlsbad, CA). Nuclear protein extraction kit was purchased from BestBio (Shanghai, China). Cholesterol assay kit and triglyceride assay kit were from Biosino Bio-technology & Science Inc. (Beijing, China). Neofect DNA transfection reagent was purchase from Neofect Biotech (Beijing, China).

2.2. Animals and treatments

Animals were housed in a thermostatic environment (24°C) with 12h light and 12h dark cycle, with access to food and water *ad libitum*. All experimental protocols were approved by the Animal Care and Use Committee of Peking University. *Lgr4*$^{flox/flox}$ mice were generated as described before (16). Albumin-Cre mice (C57BL/6J background) were purchased from Jackson Laboratory (Bar Harbor, ME). Four weeks old *Lgr4*$^{flox/flox}$ mice were fed with normal chow diet (NCD) for 8 weeks or high fat diet (HFD) for 12 weeks before injected with Ad-GFP or Ad-Cre (10^{10}pfu/mL) through tail vein to knockdown hepatic *Lgr4*. After 4 days of injection, mice were sacrificed without fasting by intraperitoneal injection of pentobarbital sodium at 70mg/kg body weight.

To generate the AL mice in which *Lgr4* is specifically deleted in hepatocytes, Albumin-Cre mice were cross-bred with *Lgr4*$^{flox/flox}$ mice. Ablation of hepatic *Lgr4* was confirmed by genotyping, quantitative RT-PCR and Western blotting. Wild type (WT) and AL mice were fed with NCD for 8 weeks or HFD for 12 weeks before sacrifice.

2.3. Isolation and culture of primary hepatocytes

Mice were anesthetized by intraperitoneal injection of pentobarbital sodium at 70mg/kg body weight. 1000IU heparin was also administrated to prevent blood coagulation. After laparotomy, the portal vein was cannulated. The liver was quickly perfused with 20mL of DHanks buffer (5mL/min) pre-warmed in 37°C water bath, followed by 30mL of 0.03% pre-warmed collagenase IV (37°C) at a flow rate of 5mL/min. Subsequently, liver was carefully removed, and hepatic tissue dispersed into serum-free high glucose DMEM medium. Cell suspension was then filtered through 80μm nylon mesh, centrifuged at 50g/min and washed twice using serum-free high glucose DMEM medium. Hepatocytes dispersed in high glucose DMEM medium containing 10% fetal calf serum (FBS) were counted and seeded in 6-well plate or 12-well plate at a concentration of 0.5–1 × 10^5 cells/mL. Cells were cultured in a humid atmosphere (5% CO_2) at 37°C for 6h to allow cell adhesion before changing to

fresh high glucose DMEM medium supplemented with 10% FBS. Hepatocytes were then infected with Ad-GFP or Ad-Cre as indicated for 48h. Where indicated, OA (125μM) was added for 24h, PA (300μM) was added for 24h, AICAR (0.5mM) or compound C (40μM) was supplied 1h before harvest.

2.4. Cell culture and shRNA transfection

AML12 cells (ATCC, Manassas, VA) were cultured in a humid atmosphere (5% CO_2) with high glucose DMEM supplemented with 10% FBS at 37°C. Cells were seeded in 12-well plate or 6-well plate until 60%~80% confluent for transfection. Cell culture medium was replaced with 950μL/well for the 12-well plate or 1.9mL/well for the 6-well plate 2h before transfection. The shRNA transfection mixture was prepared following the manufacturer's instructions. The mixture was then incubated for 18min at 37°C and added into cells at the dose of 50μl/well for the 12-well plate or 100μL/well for the 6-well plate. After 36h of incubation, culture medium was changed into high glucose DMEM supplemented with 10% FBS. Cells were then harvested or treated with OA (125μM, 24h), Rspo1 (400ng/mL, 6h) or Rspo3 (200ng/mL, 6h). shRNA sequences are listed in supplementary table 1.

2.5. Gene expression analysis

RNA was extracted using RNAtrip and reverse-transcribed into cDNAs using reverse transcription system. Quantitative real time-PCR based on SYBER Green was performed using the Agilent AriaMx real-time PCR system. Primer sequences used in this research are listed in supplementary table 2.

2.6. Western blot analysis

Cells and liver tissue were homogenized in lysis buffer. The concentration of each protein sample was determined by BCA protein quantitative kit (Applygen, Beijing, China). Protein samples were then subjected to SDS/PAGE running gel, and transferred onto nitrocellulose (NC) membrane. After incubated in 4% fat-free milk at room temperature, membranes were incubated overnight at 4°C with primary antibodies. Fluorescent secondary antibodies were used to bind with primary antibodies and visualize the expression level of specific proteins. Odyssey infrared imaging systems (LI-COR Biosciences, Lincoln, NE, USA) were used to produce graphical view of the fluorescence signals.

2.7. Measurement of triglyceride and cholesterol content

About 20mg liver tissues were homogenized in 1ml chloroform/methanol mix (2:1) on ice and kept at 4°C overnight to extract lipids into organic solution. 200μL of distilled water was added to the homogenates. The mixture was vortexed and centrifuged for 10 min at 3000rpm, 4°C. The under layer was collected using injectors, followed by desiccating with nitrogen. The lyophilized powder of lipids was resolved in 5% Triton X-100 in PBS, and the supernatant was used for lipid detection. Triglyceride and cholesterol content in liver, hepatocytes and plasma were measured according to manufacturer's instructions. Values were normalized to protein concentration or tissue weight.

2.8. Oil red O staining

The oil red staining solution was prepared and filtered before using. Frozen sections of liver were prepared and rinsed in PBS for 3 times before fixed with 4% paraformaldehyde for 10 min. After washing in PBS, slices were incubated in oil red staining solution for 1h at room temperature. Subsequently, sections were counterstained with hematoxylin for 30s and rinsed using running water for 1h. Finally, slides were mounted using 90% glycerin for observation.

2.9. Statistics

All data were expressed as mean±SEM. Statistic difference was determined by two-way ANOVA and Student's T test. $p<0.05$ was considered significant.

3. Results

3.1. Alteration of hepatic Rspo1/3 and LGR4 in response to energy status

To explore the functions of Rspos-LGR signaling in hepatic cholesterol metabolism, we firstly detected the expression of Rspos and LGRs subtypes in liver. As shown in Supplementary Figure 1A, high levels of Rspo1 and Rspo3 were detected in liver, especially Rspo3. In contrast, levels of Rspo2 and Rspo4 were negligible. The expression of LGR4 was prominently higher than its 2 homologues—LGR5 and LGR6 (Supplementary Figure 1A). Since liver is composed of multiple cell types, such as hepatocytes, Kupffer cells and hepatic stellate cells, we further determined the expression of Rspos and LGR4 in different cell types. As shown in Supplementary Figure 1B, both Rspo1 and Rspo3 are predominantly expressed in hepatocytes rather than Kupffer cells. Similarly, apart from hepatocytes, LGR4 was negligible in other cells such as Kupffer cells, macrophage cell line Raw264.7 and stellate cell line LX-2 (Supplementary Figure 1B, 1C).

We next examined the alteration of hepatic Rspo1/Rspo3 and LGR4 in response to various energy statuses. Relative to the animals fed with normal chow diet (NCD), mice fed high fat diet (HFD) showed decreased expression of *Rspo1* in liver, while the expression levels of *Rspo3* and *Lgr4* remained unaltered (Supplementary Figure 1D). Consistent with the *in vivo* results, treating primary hepatocytes with oleic acid (OA) to mimic the *in vivo* positive energy balance also down-regulated *Rspo1*, while *Rspo3* and *Lgr4* were unaffected (Supplementary Figure 1E). On the other hand, fasting significantly up-regulated *Rspo1* in liver relative to control fed group (Supplementary Figure 1F). This change was reversed upon re-feeding (Supplementary Figure 1F). *Rspo3* and *Lgr4* showed similar but less significant change relative to *Rspo1* (Supplementary Figure 1F). These results indicate that Rspos-LGR4 signaling may modulate metabolic homeostasis under different energy status.

3.2. Inhibition of hepatic cholesterol synthesis by Rspo1/3

To explore the effects of Rspo1/3-LGR4 signaling on hepatic cholesterol metabolism, we treated AML12 hepatocytes with Rspo1 or Rspo3. The optimal doses of Rspo1 or Rspo3 were determined by detecting their effects on the expression of β-catenin nuclear translocation and β-catenin target genes, a well characterized effect for Rspos-LGR4 signaling (17). As shown in Supplementary Figure 2A and 2B, 200ng/mL Rspo3 and

400ng/mL Rspo1 were proven to be effective. Both effective doses of Rspo1 and Rspo3 could reverse OA induced elevation of cholesterol content (Figure 1A). However, some previous report suggested that OA inhibits cholesterol synthesis in C6 glioma cells (18). Therefore, we also used PA to induce the accumulation of cholesterol, and found consistent results upon Rspo1 or Rspo3 stimulation (Supplementary Figure 2C). Later on, we used OA to increase cholesterol content in hepatocytes. OA increased the expression of *Srebf2*—a transcription factor crucial for cholesterol synthesis, as well as its downstream target genes, i.e., *Ldlr*, *Hmgcs1* and *Hmgcr*. Importantly, Rspo1 treatment blocked the effects of OA on these genes (Figure 1B). Further, Rspo1 decreased SREBP2 nuclear translocation (Figure 1D). The effects of Rspo3 were similar to Rspo1 (Figure 1C, 1E). These results indicate that both Rspo1 and Rspo3 could suppress hepatic cholesterol synthesis via restraining SREBP2 transcription and nuclear translocation.

3.3. Increment of cholesterol synthesis upon deficiency of hepatic LGR4

To further validate the effects of Rspos-LGR4 signaling on hepatic cholesterol metabolism, we constructed *Lgr4*$^{flox/flox}$ mice and knocked down hepatic LGR4 through tail vein injection of Cre adenovirus (Ad-Cre). After 4 days of Ad-Cre injection, the expression of *Lgr4* in liver was significantly restrained compared with control group injected with GFP adenovirus (Ad-GFP) (Supplementary Figure 3A). We also confirmed both NCD and HFD *Lgr4*$^{flox/flox}$ mice displayed decreased hepatic LGR4 protein expression after Ad-Cre injection (Supplementary Figure 3B). 4-weeks old *Lgr4*$^{flox/flox}$ mice were fed with NCD for 8 weeks, then divided into 2 groups randomly and injected with Ad-GFP or Ad-Cre. Body weight and tissue weights of hepatic *Lgr4* knockdown (*Lgr4*^{LKO}) mice was unchanged relative to their littermate (Supplementary Figure 3C). Histochemistry and Oil red O staining also showed no significant differences between 2 groups (Supplementary Figure 3E, F). However, the hepatic cholesterol content of *Lgr4*^{LKO} mice was 1.5 fold of *Lgr4*$^{flox/flox}$ mice (Figure 2A). No significant change of serum cholesterol, serum and hepatic triglyceride was observed between two groups (Figure 2A). *Srebf2* was induced in *Lgr4*^{LKO} mice (Figure 2B). This change was associated with a significant increase of SREBP2 nuclear translocation (Figure 2E). Consistently, *Srebf2* target genes *Ldlr*, *Hmgcs1* and *Hmgcr* were significantly up-regulated (Figure 2B).

We next examined the impacts of hepatic LGR4 deletion on cholesterol synthesis under HFD condition. 4-weeks old *Lgr4*$^{flox/flox}$ mice were fed with HFD for 12 weeks, followed by Ad-Cre or Ad-GFP injection. After 4 days of injection, no significant difference was observed between *Lgr4*$^{flox/flox}$ and *Lgr4*^{LKO} mice with regard to body weight and tissue weights (Supplementary Figure 3D). Histochemistry and Oil red O staining showed increased lipid in liver of *Lgr4*^{LKO} mice compared with *Lgr4*$^{flox/flox}$ mice (Supplementary Figure 3G, H). Consistently, hepatic cholesterol and triglyceride contents of *Lgr4*^{LKO} mice increased by 2 folds relative to *Lgr4*$^{flox/flox}$ mice, while serum cholesterol and triglyceride levels remained unaltered (Figure 2C). Under HFD condition, *Lgr4* deficiency resulted in increase of *Srebf2* and its target genes, including *Ldlr*, *Hmgcs1* and *Hmgcr* (Figure 2D). SREBP2 nuclear translocation in liver of HFD *Lgr4*^{LKO} mice was enhanced (Figure 2F). Thus, transient ablation of hepatic *Lgr4* in mice fed either NCD or HFD enhanced

expression and nuclear translocation of *Srebf2* as well as its downstream targets, leading to subsequent increase of cholesterol synthesis.

We next examined the effect of stable deficiency of *Lgr4* on hepatic cholesterol metabolism using the hepatic specific *Lgr4* knockout mice (AL). *Lgr4*$^{flox/flox}$ littermates (WT) were used as control. As shown in Supplementary Figure 4A, body weight and most of the tissue weight were comparable between WT and AL mice fed NCD. Liver weight of AL mice slightly reduced accompanied with decreased expression of LGR4 protein in liver (Supplementary Figure 4A, C). Histochemistry staining showed hepatocyte vacuolization of AL mice (Supplementary Figure 4D). However, Oil red O staining was comparable between 2 groups (Supplementary Figure 4E). Hepatic cholesterol content in AL mice elevated relative to WT mice, whereas no significant increase in hepatic triglyceride levels was observed (Figure 3A). Serum levels of cholesterol and triglyceride also increased compared with the littermates (Figure 3A). Hepatic mRNA levels of *Lgr4* decreased as expected, whereas levels of *Srebf2*, *Hmgcs1* and *Hmgcr* significantly increased in AL mice (Figure 3B). Consistent with the change at mRNA level, hepatic *Lgr4* ablation enhanced translocation of SREBP2 into nuclei (Figure 3E). Similar results were observed for AL mice fed HFD. After 12 weeks of HFD, liver weight and hepatic LGR4 expression of AL mice decreased, while body weights of AL and WT mice were identical (Supplementary Figure 4B, C). Although the histochemistry staining showed no significant changes, there was increased accumulation of perivascular lipid in the liver of AL mice (Supplementary Figure 4F, G). In comparison to WT mice, AL mice demonstrated a significant increase in hepatic and serum levels of cholesterol and triglyceride (Figure 3C). Deficiency of *Lgr4* boosted transcription of *Srebf2* (Figure 3D) and its subsequent nuclear translocation (Figure 3F) in AL mice fed HFD. Associated with the change of SREBP2, its downstream target genes significantly up-regulated, such as *Pcsk9*, *Hmgcs1* and *Hmgcr* (Figure 3D).

In summary, either transient or stable ablation of hepatic LGR4 in mice fed NCD or HFD promotes cholesterol synthesis, SREBP2 transcription and nuclear translocation, expression of genes relevant to cholesterol synthesis.

3.4. Cell-autonomous effect of hepatic LGR4 deficiency

To verify that the effects of LGR4 deficiency on hepatic cholesterol synthesis are cell-autonomous, we isolated primary hepatocytes from *Lgr4*$^{flox/flox}$ mice and knocked down *Lgr4* through Ad-Cre administration. Primary hepatocytes of *Lgr4*$^{flox/flox}$ mice were treated with Ad-GFP or Ad-Cre for indicated times. After 48h of treatment, LGR4 mRNA and protein were both effectively suppressed (Figure 4A, 4B). LGR4 deficiency promoted cholesterol deposition in hepatocytes under conditions treated with or without OA (Figure 4C). Increase of triglyceride content in hepatocytes was only observed after OA stimulation in LGR4 deficient hepatocytes (Figure 4C). These changes were associated with an increase of genes relevant to cholesterol metabolism such as *Pcsk9*, *Ldlr*, *Srebf2*, *Hmgcs1* and *Hmgcr* (Figure 4D). LGR4 deficient hepatocytes showed remarkable increase of SREBP2 translocation into nuclei (Figure 4E).

3.5. AMPKα dependent mechanism

Adenosine monophosphate (AMP)-activated protein kinase (AMPK) is one of the pivotal energy-sensing molecules expressed in almost all eukaryotic cells. Numerous studies have confirmed that AMPK is critical for the cellular energy metabolism such as GLUT4 membrane translocation, fatty acid β oxidation, mitochondrial biogenesis and autophagy (19). Studies from ours and others have demonstrated that AMPK directly phosphorylates SREBP2 precursor, leading to the reduction of SREBP2 nuclear translocation (6, 20, 21). We thus examined the effects of Rspo1/3-LGR4 signaling on AMPK. As shown in Figure 5A, both Rspo1 and Rspo3 stimulation potentiated phosphorylation of Thr172 site of AMPKα in AML12 cells, indicating AMPK activation. Compound C is commonly used as an AMPK antagonist. As presented in Supplementary Figure 5A, incubation of AML12 cells with compound C for 1h dose-dependently reduced phosphorylation of AMPKα Thr172. Rspo1 and Rspo3 significantly attenuated OA induced elevation of cholesterol content in AML12 cells (Figure 5B). This effect was blunted by compound C (Figure 5B). Compound C significantly attenuated the Rspo1 induced activation of AMPKα and subsequent suppression of cholesterol metabolism relevant genes including *Srebf2*, *Ldlr*, *Hmgcs1* and *Hmgcr*, as well as the nuclear translocation of SREBP2 in hepatocytes treated with OA (Figure 5C, 5D). Similarly, compound C abolished the effects of Rspo3 on AMPKα, cholesterol metabolism relevant genes, and the SREBP2 nuclear translocation (Figure 5E, 5F).

In *Lgr4*$^{flox/flox}$ mice fed NCD and HFD, transient knockdown of hepatic LGR4 using Ad-Cre resulted in reduced activation of AMPKα (Figure 6A). Similarly, phosphorylation of AMPKα in liver with stable deletion of LGR4 (AL mice) significantly declined compared with WT mice (Figure 6A). *In vitro*, knockdown LGR4 in *Lgr4*$^{flox/flox}$ hepatocytes using Ad-Cre suppressed activation of AMPKα as well (Figure 6B). We then tested if AMPKα agonist AICAR could reverse the changes driven by LGR4 depletion. In AML12 cells, AICAR dose-dependently potentiated AMPKα phosphorylation at Thr172 site (Supplementary Figure 5B). Activation of AMPKα by AICAR significantly attenuated the increase of hepatic cholesterol content in LGR4 deficient hepatocytes treated with or without OA (Figure 6C). Consistently, AICAR abolished the up-regulation of *Srebf2* and its target genes including *Ldlr*, *Hmgcs1* and *Hmgcr* induced by LGR4 deletion (Figure 6D). Additionally, AICAR treatment was sufficient to block the SREBP2 nuclear translocation induced by LGR4 ablation (Figure 6E).

Two isoforms of AMPKα have been identified to date, namely, AMPKα1 and AMPKα2 (22). To explore the isoform mediating the downstream effects of Rspo1/3-LGR4 signaling, we constructed shRNA specifically interfering AMPKα1 or AMPKα2. AML12 cells transfected with AMPKα1 shRNA for 36h demonstrated a significant reduction in the levels of AMPKα1, while AMPKα2 levels were unaffected (Figure 7A). Remarkably, AMPKα1 deficiency abrogated the inhibitory effects of Rspo1 on cholesterol synthesis (Figure 7A), mRNA levels of *Srebf2*, *Ldlr*, *Hmgcs1* and *Hmgcr* (Figure 7B), as well as nuclear translocation of SREBP2 (Figure 7C). AMPKα1 deficiency reduced the Rspo1-induced upregulation of AMPKα phosphorylation (Figure 7C). Similar results were also found upon Rspo3 stimulation (Supplementary Figure 6A–C).

As shown in Figure 7D, AML12 cells transfected with AMPKα2 shRNA for 36h significantly reduced the expression level of AMPKα2 without affecting AMPKα1. Much alike AMPKα1 knockdown, AMPKα2 deletion also reversed the decrease of cholesterol level (Figure 7D), mRNA levels of cholesterol metabolism relevant genes such as *Srebf2*, *Ldlr*, *Hmgcs1* and *Hmgcr* (Figure 7E), and nuclear translocation of SREBP2 (Figure 7F) in hepatocytes treated with Rspo1. Silence of AMPKα2 gene significantly attenuated the increase of AMPKα phosphorylation induced by Rspo1 (Figure 7F). Much like Rspo1, AMPKα2 knockdown hepatocytes displayed similar results under Rspo3 treatment (Supplementary Figure 6D–F).

Hepatocytes with double-knockdown of AMPKα1 and AMPKα2 were resistant to Rspo1 or Rspo3 induced decline of cholesterol level (Supplementary Figure 7A, 7B). The effects of Rspo1 and Rspo3 on cholesterol metabolism relevant genes such as *Srebf2*, *Ldlr*, *Hmgcs1*, *Hmgcr* were significantly blunted in hepatocytes with ablation of both AMPKα1 and AMPKα2 (Supplementary Figure 7C, 7D). Likewise, the inhibitory effects of Rspo1 and Rspo3 on SREBP2 nuclear translocation were apparently abolished in hepatocytes with deficiency of both AMPKα1 and AMPKα2 (Supplementary Figure 7E, 7F).

4. Discussion

Rspos-LGR4 signaling has been demonstrated to be critical for embryogenesis and maintenance of stem cell functions. The present study reveals a pivotal role for this signaling pathway in the cholesterol homeostasis. The highlights of our study are as follows: (1) Rspo1/3 inhibits hepatic cholesterol synthesis, while LGR4 deficiency increases cholesterol contents in hepatocytes; (2) Rspo1/3 activates AMPKα, and subsequently blocks the transcriptional activation of *Srebf2* and the SREBP2 nuclear translocation, leading to the suppression of its target genes involved in cholesterol synthesis, while deletion of hepatic LGR4 induced opposite effects; (3) Both pharmacological or genetic intervention of AMPKα reverse the inhibitory effects of Rspo1 and Rspo3 on hepatic cholesterol synthesis. Our study thus demonstrates that Rspo1/3-LGR4 signaling inhibits hepatic cholesterol synthesis through a mechanism dependent on the AMPK-SREBP2 pathway (Figure 8).

Being mainly expressed in the stem cells, LGR4 is critical for the maintenance of stem cells and thus for the embryonic development (11). Our finding extends the physiological function of LGR4 to the cholesterol homeostasis. Conflicting results have been reported on the metabolic function of LGR4. In hypothalamus, activation of LGR4 by R-spondin 1 or 3 inhibits food intake (23). In contrast, mice with global ablation of LGR4 show decrement in adiposity and resistance to dietary and leptin mutant-induced obesity, due to enhanced browning of white adipose tissues (14). Consistently, human genetic analysis has identified the gain-of-function variant of LGR4, LGR4 A750T variant, as a genetic determinant of central obesity (24). All these studies suggest that LGR4 may either function as an anorexic signal through the central hypothalamus or as a stimulator for energy expenditure through peripheral adipose tissues to promote negative or positive energy balance respectively. Thus, conditional manipulation of LGR4 in distinct cells such as hypothalamic neurons, adipocytes, hepatocytes and islet cells is a critical precondition to dissect the differential action of this molecule on energy homeostasis. Using the *in vivo* and *in vitro* approach to

specifically manipulate the expression of LGR4 gene in hepatocytes, we reveal an additional physiological function for LGR4 in cholesterol metabolism. Activation of LGR4 in hepatocytes by R-spondin1 or 3 attenuated cholesterol synthesis, whereas deficiency of LGR4 in hepatocytes significantly increased the synthesis of cholesterol both in mice and in cultured hepatocytes. The reduction of hepatic cholesterol upon activation of LGR4 may occur through the attenuation of cholesterol synthesis. Our study thus establishes Rspo1/3-LGR4 signaling as a novel endogenous system contributing to the cholesterol homeostasis. Targeting the Rspos-LGR4 signaling in hepatocytes may provide an alternative strategy for the intervention of cholesterol dysfunction including hypercholesterolemia.

The intracellular signaling pathway mediating the physiological function of Rspos-LGR4 remains largely unknown. Previous study has suggested that Rspos-LGR4 functions to potentiate Wnt/β-catenin signaling (17). We have identified AMPK-SREBP2 as the downstream mediators of Rspo1/3-LGR4 signaling in the control of hepatic cholesterol synthesis. Both pharmacological and genetic intervention of AMPKα reversed the decrement of SREBP2 nuclear translocation induced by Rspo1/3 and suppressed cholesterol synthesis. Conversely, AMPKα agonist abolished enhancement of cholesterol synthesis in context of LGR4 ablation. Furthermore, both isoforms of AMPKα are required for the suppression of hepatic cholesterol synthesis induced by Rspo1/3-LGR4 signaling.

How Rspo1/3-LGR4 signaling activates AMPKα remains unclear. Having been extensively verified, the major function of Rspos-LGR4 pathway is to potentiate Wnt/β-catenin signaling. Accordingly, we assume that Wnt/β-catenin axis may be responsible for ectopic activation of AMPKα. Glycogen synthase kinase 3β (GSK3β) negatively regulates Wnt/β-catenin signaling through accelerating degradation of β-catenin. Previous studies have demonstrated that GSK3β acts as a potent inhibitor of AMPK activation (25, 26). Further study is required to determine whether GSK3β is involved in Rspos-LGR4 stimulated AMPK phosphorylation in hepatocytes.

In summary, our study demonstrates that in liver, Rspos-LGR4 signaling functions as a crucial endogenous pathway to inhibit cholesterol synthesis through suppressing SREBP2 as well as its downstream targets. This function of Rspos-LGR4 axis is mediated by AMPKα. Considering that elevation of cholesterol in liver is critical for the progression from NAFL to NASH, our finding suggests that Rspos-LGR4 axis may provide novel therapeutic targets for NAFLD.

Supplementary Material

Refer to Web version on PubMed Central for supplementary material.

Acknowledgements

This research was supported by grants from the National Key R&D Program of China (2017YFC0908900), the National Natural Science Foundation of China (81730020, 81930015) and National Institutes of Health Grant 1R01DK110273 and R01DK112755.

Abbreviations

Rspos	R-spondins
LGR4	leucine-rich repeat G-protein-coupled receptor 4
AMP	adenosine 5’-monophosphate
AMPKα	AMP activated protein kinase α
NAFLD	non-alcoholic fatty liver disease
NAFL	non-alcoholic fatty liver
NASH	non-alcoholic steatohepatitis
SREBP2	sterol regulatory element binding protein 2
ER	endoplasmic reticulum
SCAP	SREBP cleavage activation protein
Insig	insulin induced gene
S1P	Site-1 protease
S2P	Site-2 protease
SREBP2-N	SREBP2 N terminus
SRE	sterol regulatory element
NCD	normal chow diet
HFD	high fat diet
WT	wild type
FBS	fetal calf serum
NC	nitrocellulose
OA	oleic acid
PA	palmitic acid
GSK3β	glycogen synthase kinase 3β

7. References

1. Masuoka HC, and Chalasani N (2013) Nonalcoholic fatty liver disease: an emerging threat to obese and diabetic individuals. Ann. N. Y. Acad. Sci 1281, 106–122 [PubMed: 23363012]
2. Min HK, Kapoor A, Fuchs M, Mirshahi F, Zhou H, Maher J, Kellum J, Warnick R, Contos MJ, and Sanyal AJ (2012) Increased hepatic synthesis and dysregulation of cholesterol metabolism is associated with the severity of nonalcoholic fatty liver disease. Cell Metab. 15, 665–74 [PubMed: 22560219]

3. Puri P, Baillie RA, Wiest MM, Mirshahi F, Choudhury J, Cheung O, Sargeant C, Contos MJ, and Sanyal AJ (2007) A lipidomic analysis of nonalcoholic fatty liver disease. Hepatology 46, 1081–90 [PubMed: 17654743]
4. Dongiovanni P, Petta S, Mannisto V, Mancina RM, Pipitone R, Karja V, Maggioni M, Kakela P, Wiklund O, Mozzi E, Grimaudo S, Kaminska D, Rametta R, Craxi A, Fargion S, Nobili V, Romeo S, Pihlajamaki J, and Valenti L (2015) Statin use and non-alcoholic steatohepatitis in at risk individuals. J. Hepatol 63, 705–12 [PubMed: 25980762]
5. Yoneda M, Fujita K, Nozaki Y, Endo H, Takahashi H, Hosono K, Suzuki K, Mawatari H, Kirikoshi H, Inamori M, Saito S, Iwasaki T, Terauchi Y, Kubota K, Maeyama S, and Nakajima A (2010) Efficacy of ezetimibe for the treatment of non-alcoholic steatohepatitis: an open-label, pilot study. Hepatol. Res 40, 566–73 [PubMed: 20412324]
6. Tang H, Yu R, Liu S, Huwatibieke B, Li Z, and Zhang W (2016) Irisin inhibits hepatic cholesterol synthesis via AMPK-SREBP2 signaling. EBioMedicine 6, 139–148 [PubMed: 27211556]
7. Goldstein JL, DeBose-Boyd RA, and Brown MS (2006) Protein sensors for membrane sterols. Cell 124, 35–46 [PubMed: 16413480]
8. Nagoshi E, Imamoto N, Sato R, Yoneda Y (1999) Nuclear import of sterol regulatory element-binding protein-2, a basic helix-loop-helix-leucine zipper (bHLH-Zip)-containing transcription factor, occurs through the direct interaction of importinβ with HLHZip. Mol. Biol. Cell 10, 2221–33 [PubMed: 10397761]
9. Yi J, Xiong W, Gong X, Bellister S, Ellis LM, and Liu Q (2013) Analysis of LGR4 receptor distribution in human and mouse tissues. PLoS One 8, e78144 [PubMed: 24205130]
10. Mazerbourg S, Bouley DM, Sudo S, Klein CA, Zhang JV, Kawamura K, Goodrich LV, Rayburn H, Tessier-Lavigne M, and Hsueh AJ (2004) Leucine-rich repeat-containing, G protein-coupled receptor 4 null mice exhibit intrauterine growth retardation associated with embryonic and perinatal lethality. Mol. Endocrinol 18, 2241–54 [PubMed: 15192078]
11. Li Z, Zhang W, and Mulholland MW (2015) LGR4 and Its Role in Intestinal Protection and Energy Metabolism. Front. Endocrinol. (Lausanne) 6, 131 [PubMed: 26379625]
12. Gao Y, Kitagawa K, Hiramatsu Y, Kikuchi H, Isobe T, Shimada M, Uchida C, Hattori T, Oda T, Nakayama K, Nakayama KI, Tanaka T, Konno H, and Kitagawa M (2006) Up-regulation of GPR48 induced by down-regulation of p27Kip1 enhances carcinoma cell invasiveness and metastasis. Cancer Res. 66, 11623–31 [PubMed: 17178856]
13. Sun Y, Hong J, Chen M, Ke Y, Zhao S, Liu W, Ma Q, Shi J, Zou Y, Ning T, Zhang Z, Liu R, Wang J, and Ning G (2015) Ablation of Lgr4 enhances energy adaptation in skeletal muscle via activation of Ampk/Sirt1/Pgc1α pathway. Biochem. Biophys. Res. Commun 464, 396–400 [PubMed: 26102032]
14. Wang J, Liu R, Wang F, Hong J, Li X, Chen M, Ke Y, Zhang X, Ma Q, Wang R, Shi J, Cui B, Gu W, Zhang Y, Zhang Z, Wang W, Xia X, Liu M, and Ning G (2013) Ablation of LGR4 promotes energy expenditure by driving white-to-brown fat switch. Nat. Cell Biol 15, 1455–63 [PubMed: 24212090]
15. Wang F, Zhang X, Wang J, Chen M, Fan N, Ma Q, Liu R, Wang R, Li X, Liu M, and Ning G (2014) LGR4 acts as a link between the peripheral circadian clock and lipid metabolism in liver. J. Mol. Endocrinol 52, 133–43 [PubMed: 24353284]
16. Li Z, Liu S, Lou J, Mulholland M, and Zhang W (2019) LGR4 protects hepatocytes from injury in mouse. Am. J. Physiol. Gastrointest. Liver Physiol 316, G123–G131 [PubMed: 30406697]
17. de Lau W, Peng WC, Gros P, and Clevers H (2014) The R-spondin/Lgr5/Rnf43 module: regulator of Wnt signal strength. Genes Dev. 28, 305–16 [PubMed: 24532711]
18. Natali F, Siculella L, Salvati S, and Gnoni GV (2007) Oleic acid is a potent inhibitor of fatty acid and cholesterol synthesis in C6 glioma cells. J. Lipid Res 48, 1966–75 [PubMed: 17568062]
19. Hardie DG, Ross FA, and Hawley SA (2012) AMPK: a nutrient and energy sensor that maintains energy homeostasis. Nat. Rev. Mol. Cell Biol 13, 251–62 [PubMed: 22436748]
20. Li Y, Xu S, Mihaylova MM, Zheng B, Hou X, Jiang B, Park O, Luo Z, Lefai E, Shyy JY, Gao B, Wierzbicki M, Verbeuren TJ, Shaw RJ, Cohen RA, and Zang M (2011) AMPK phosphorylates and inhibits SREBP activity to attenuate hepatic steatosis and atherosclerosis in diet-induced insulin-resistant mice. Cell Metab. 13, 376–388 [PubMed: 21459323]

21. Liu S, Jing F, Yu C, Gao L, Qin Y, and Zhao J (2015) AICAR-induced activation of AMPK inhibits TSH/SREBP-2/HMGCR pathway in liver. PLoS One 10, e0124951 [PubMed: 25933205]

22. Hardie DG (2007) AMP-activated/SNF1 protein kinases: conserved guardians of cellular energy. Nat. Rev. Mol. Cell Biol 8, 774–85 [PubMed: 17712357]

23. Li JY, Chai B, Zhang W, Fritze DM, Zhang C, and Mulholland MW (2014) LGR4 and its ligands, R-spondin 1 and R-spondin 3, regulate food intake in the hypothalamus of male rats. Endocrinology 155, 429–40 [PubMed: 24280058]

24. Zou Y, Ning T, Shi J, Chen M, Ding L, Huang Y, Kauderer S, Xu M, Cui B, Bi Y, Liu S, Hong J, Liu R, Ning G, and Wang J (2017) Association of a gain-of-function variant in LGR4 with central obesity. Obesity 25, 252–260 [PubMed: 27925416]

25. Zhou H, Wang H, Ni M, Yue S, Xia Y, Busuttil RW, Kupiec-Weglinski JW, Lu L, Wang X, Zhai Y (2018) Glycogen synthase kinase 3β promotes liver innate immune activation by restraining AMP-activated protein kinase activation. J. Hepatol 69, 99–109 [PubMed: 29452207]

26. Suzuki T, Bridges D, Nakada D, Skiniotis G, Morrison SJ, Lin JD, Saltiel AR, Inoki K (2013) Inhibition of AMPK catabolic action by GSK3. Mol. Cell 50, 407–19 [PubMed: 23623684]

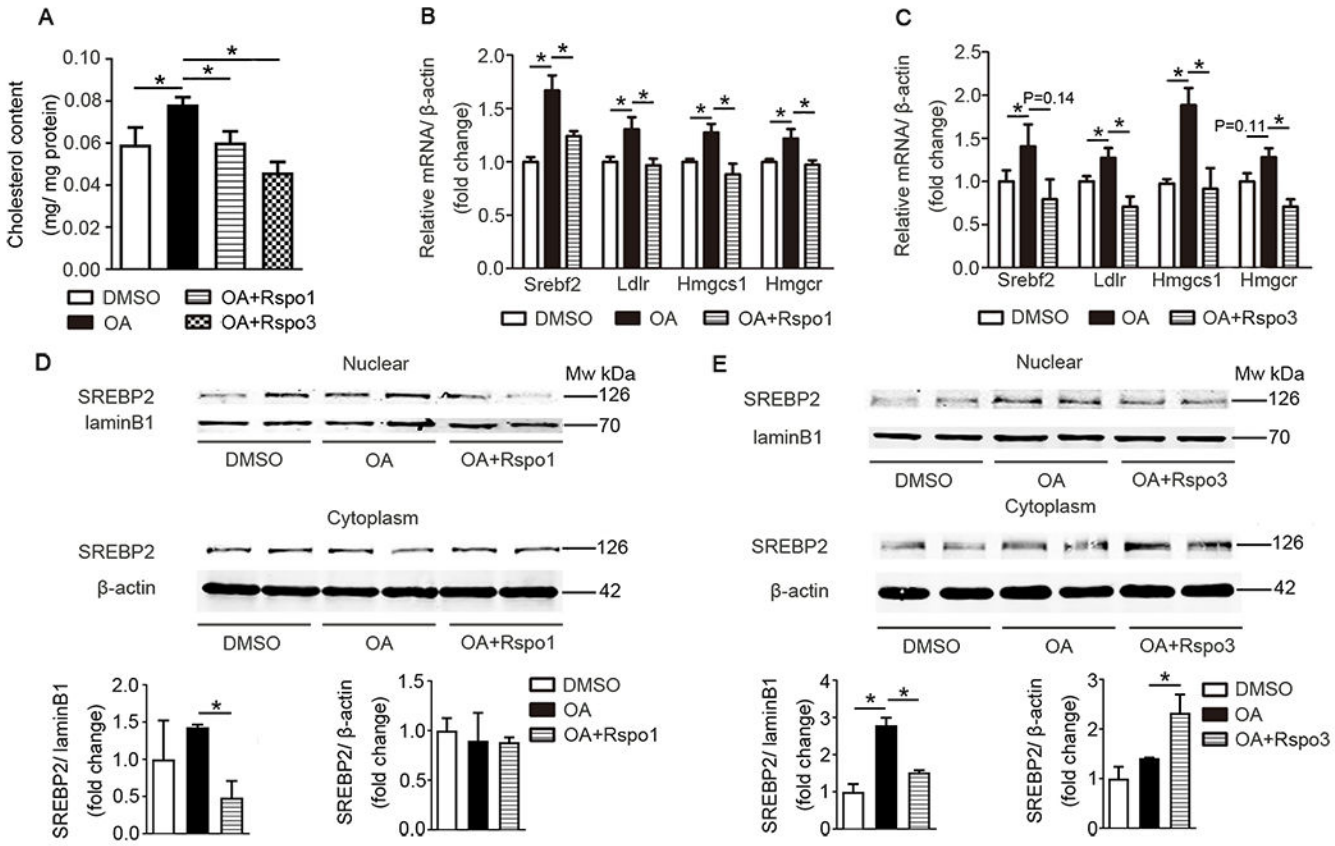

Figure 1. Inhibition of hepatic cholesterol synthesis by Rspo1/3.

A. Cholesterol content in AML12 cells under different treatments. AML12 cells were treated with OA (125μM) for 24h, followed by 6h incubation with Rspo1 or Rspo3. Cholesterol contents were determined using assay kits. n=4.

B. Rspo1 repressed expression of genes related to cholesterol uptake and synthesis upon OA treatment. Hepatic mRNAs were extracted and analyzed by quantitive RT-PCR. n=6.

C. Rspo3 repressed expression of genes related to cholesterol uptake and synthesis upon OA treatment. Hepatic mRNAs were extracted and analyzed by quantitive RT-PCR. n=6.

D. Rspo1 reversed SREBP2 nuclear translocation induced by OA. Western blotting was performed to detect protein level of SREBP2 in nucleus and cytoplasm. The relative expression level of SREBP2 was calculated using Image J software. Shown is the representative of at least 3 repeat experiments.

E. Rspo3 reversed SREBP2 nuclear translocation induced by OA. Western blotting was performed to detect protein level of SREBP2 in nucleus and cytoplasm. The relative expression level of SREBP2 was calculated using Image J software. Shown is the representative of at least 3 repeat experiments.

Data are represented as mean±SEM. *p<0.05.

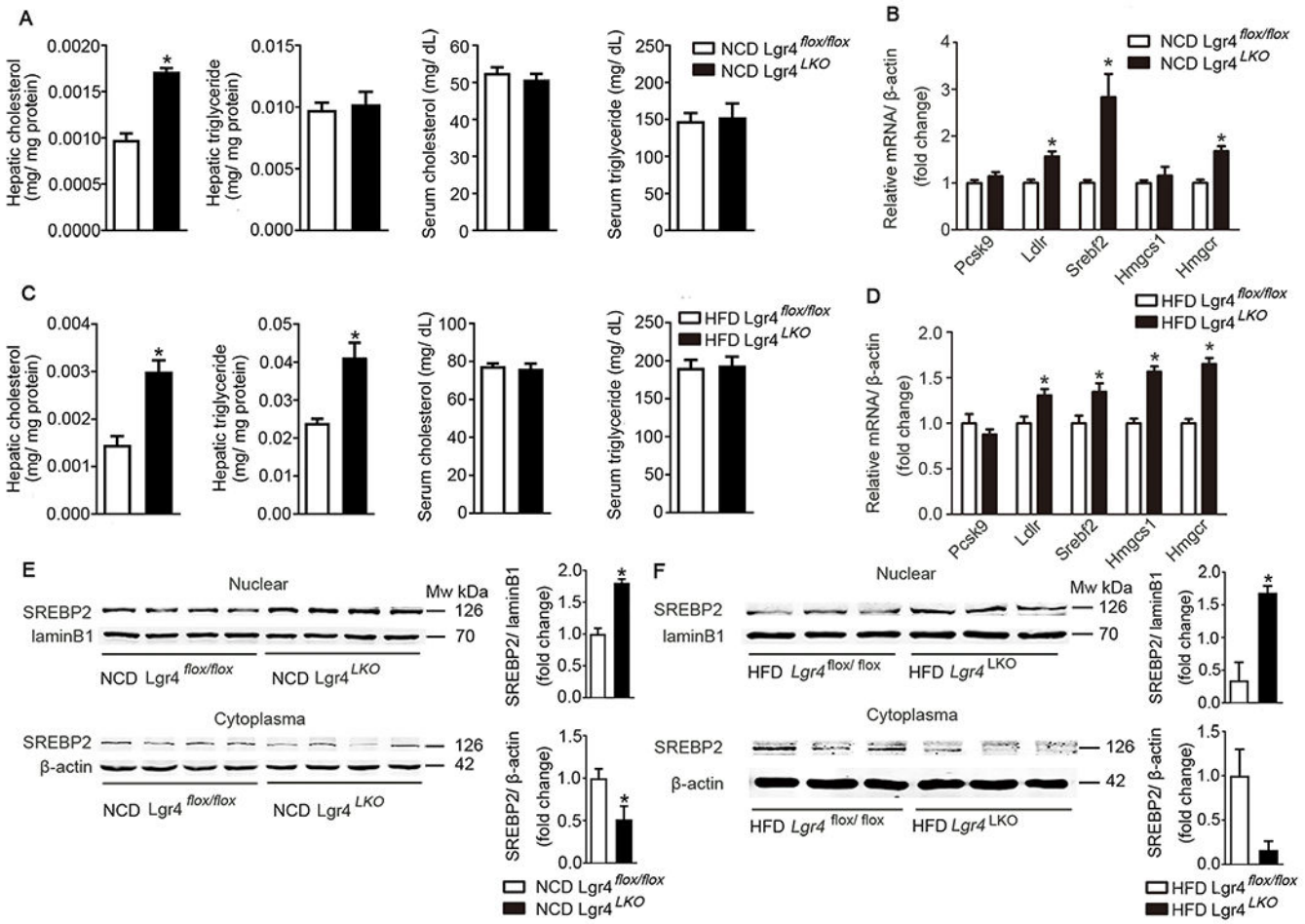

Figure 2. Increment of cholesterol synthesis upon hepatic LGR4 knockdown using Ad-Cre.

A. NCD *Lgr4*^{LKO} mice displayed increased hepatic cholesterol content. Hepatic and serum cholesterol, triglyceride contents were measured by assay kits. n=6.

B. Upregulation of genes related to cholesterol uptake and synthesis in liver of NCD *Lgr4*^{LKO} mice. Hepatic mRNAs were extracted and analyzed by quantitive RT-PCR. n=6.

C. Increased hepatic cholesterol and triglyceride contents in HFD *Lgr4*^{LKO} mice. Hepatic and serum triglyceride and cholesterol contents were measured by assay kits. n=6.

D. Upregulation of genes related to cholesterol uptake and synthesis in liver of HFD *Lgr4*^{LKO} mice. Hepatic mRNAs were extracted and analyzed by quantitive RT-PCR. n=6.

E. Increased hepatic SREBP2 nuclear translocation in NCD *Lgr4*^{LKO} mice. Western blotting was performed to detect protein level of SREBP2 in nucleus and cytoplasm. The relative expression level of SREBP2 was calculated using Image J software. Shown is the representative of at least 3 repeat experiments.

F. Increased hepatic SREBP2 nuclear translocation in HFD *Lgr4*^{LKO} mice. Western blotting was performed to detect protein level of SREBP2 in nucleus and cytoplasm. The relative expression level of SREBP2 was calculated using Image J software. Shown is the representative of at least 3 repeat experiments.

Data are represented as mean±SEM. *p<0.05.

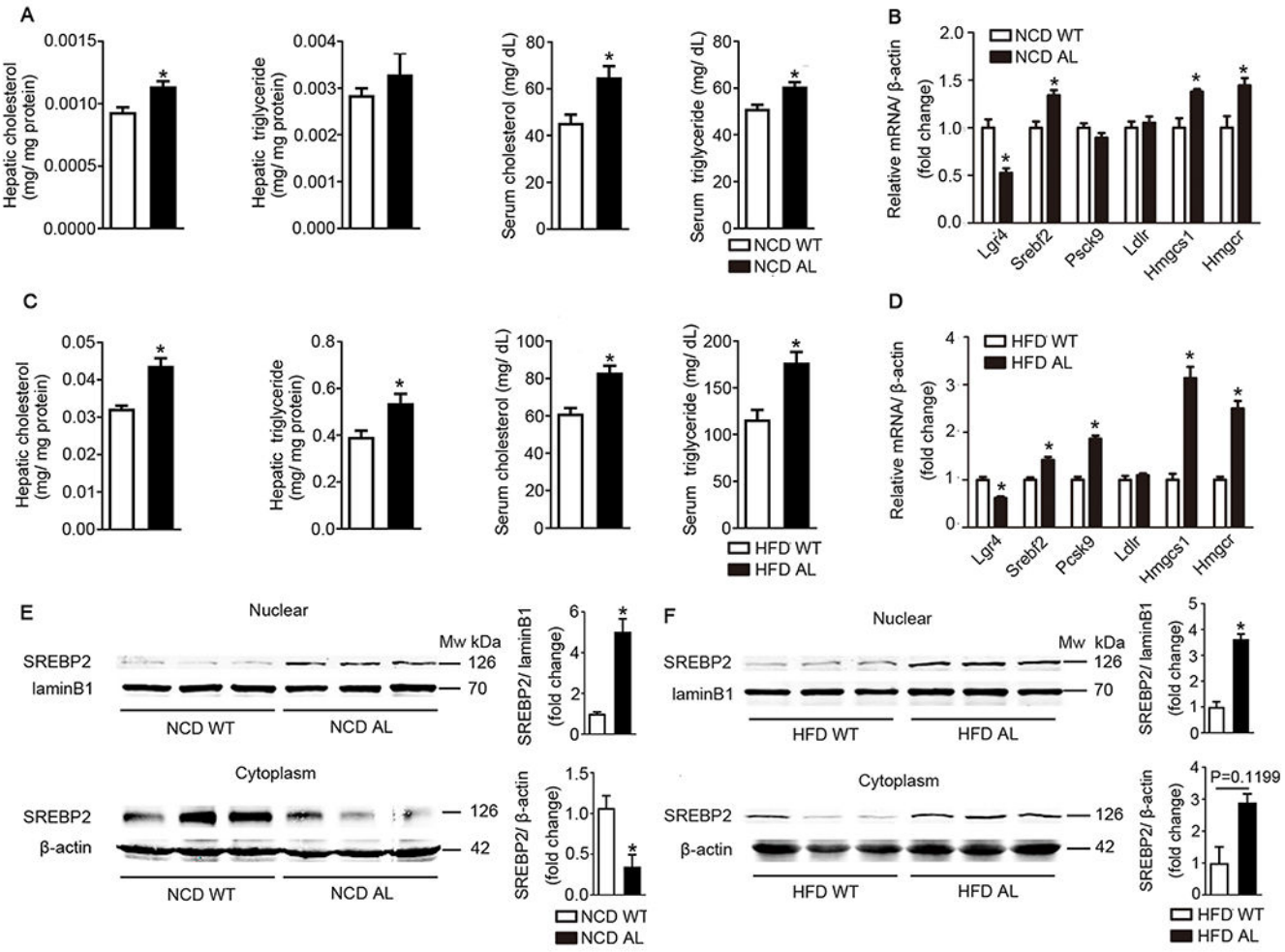

Figure 3. Hepatic stable deficiency of *Lgr4* promoted cholesterol synthesis.

4-weeks old hepatic specific LGR4 deficient mice (AL mice) and their *Lgr4*$^{flox/flox}$ littermate (WT mice) were fed with normal chow diet for 8 weeks or high fat diet for 12 weeks before sacrifice.

A. Elevated hepatic cholesterol and serum cholesterol, triglyceride level of NCD AL mice compared with WT mice. Hepatic and serum cholesterol, triglyceride contents were measured by assay kits. n=6.

B. Hepatic specific *Lgr4* knockdown increased cholesterol uptake and synthesis of NCD mice. Hepatic mRNAs were extracted and analyzed by quantitive RT-PCR. n=6.

C. Elevated hepatic and serum cholesterol, triglyceride level of HFD AL mice compared with WT mice. Hepatic and serum cholesterol, triglyceride contents were measured by assay kits. n=6.

D. Hepatic specific LGR4 knockdown increased cholesterol uptake and synthesis of HFD mice. Hepatic mRNAs were extracted and analyzed by quantitive RT-PCR. n=6.

E. Hepatic specific *Lgr4* knockdown increases nuclear translocation of SREBP2 of NCD mice. Western blotting was performed to detect protein level of SREBP2 in nucleus and cytoplasm. The relative expression level of SREBP2 was calculated using Image J software. Shown is the representative of at least 3 repeat experiments.

F. Hepatic specific LGR4 knockdown increases expression of SREBP2 of HFD mice. Western blotting was performed to detect protein level of SREBP2 in nucleus and cytoplasm. The relative expression level of SREBP2 was calculated using Image J software. Shown is the representative of at least 3 repeat experiments.
Data are represented as mean±SEM. *p<0.05.

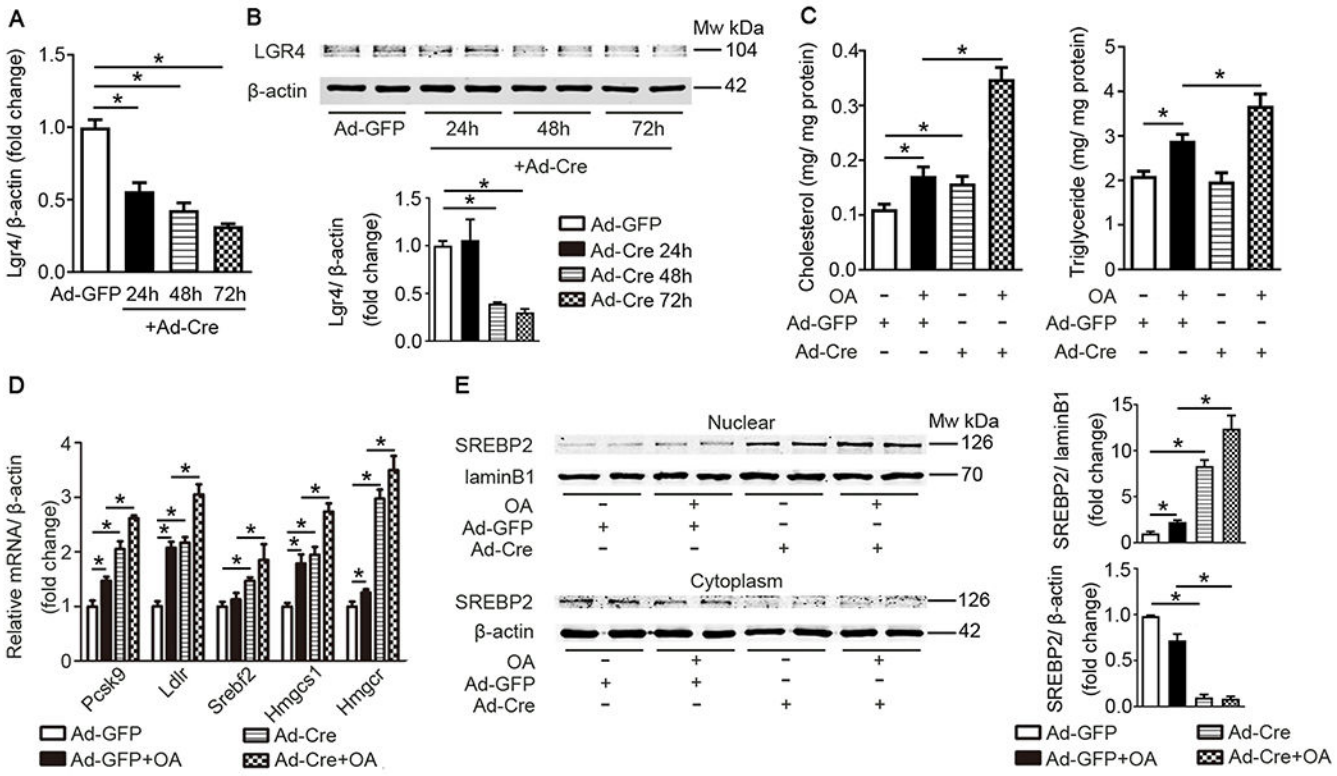

Figure 4. Cell-autonomous effect of hepatic LGR4 deficiency.

A. Ad-Cre induced *Lgr4* knockdown in *Lgr4*$^{flox/flox}$ primary hepatocytes. Primary hepatocytes from *Lgr4*$^{flox/flox}$ mice were isolated and infected with Ad-GFP or Ad-Cre(10^8pfu/mL) for indicated time. mRNAs were extracted and analyzed by quantitive RT-PCR. n=6.

B. Ad-Cre suppressed expression of LGR4 protein in *Lgr4*$^{flox/flox}$ primary hepatocytes. Western blotting was performed to detect protein level of LGR4. The relative expression level of LGR4 was calculated using Image J software. Shown is the representative of at least 3 repeat experiments.

C. LGR4 deficiency of hepatocytes increases cholesterol content. *Lgr4*$^{flox/flox}$ primary hepatocytes were incubated with Ad-Cre or Ad-GFP for 48h, followed by 24h of OA or DMSO treatment. Cholesterol and triglyceride content in hepatocytes were then determined after different treatment by assay kits. n=6.

D. LGR4 deficiency of hepatocytes increases cholesterol uptake and synthesis. After indicated treatments, mRNA was extracted from primary hepatocytes and analyzed by quantitive RT-PCR. n=6.

E. LGR4 deficiency of hepatocytes increases nuclear translocation of SREBP2. After indicated treatments, western blotting was performed to detect protein level of SREBP2 in nucleus and cytoplasm. The relative expression level of SREBP2 was calculated using Image J software. Shown is the representative of at least 3 repeat experiments.

Data are represented as mean±SEM. *p<0.05.

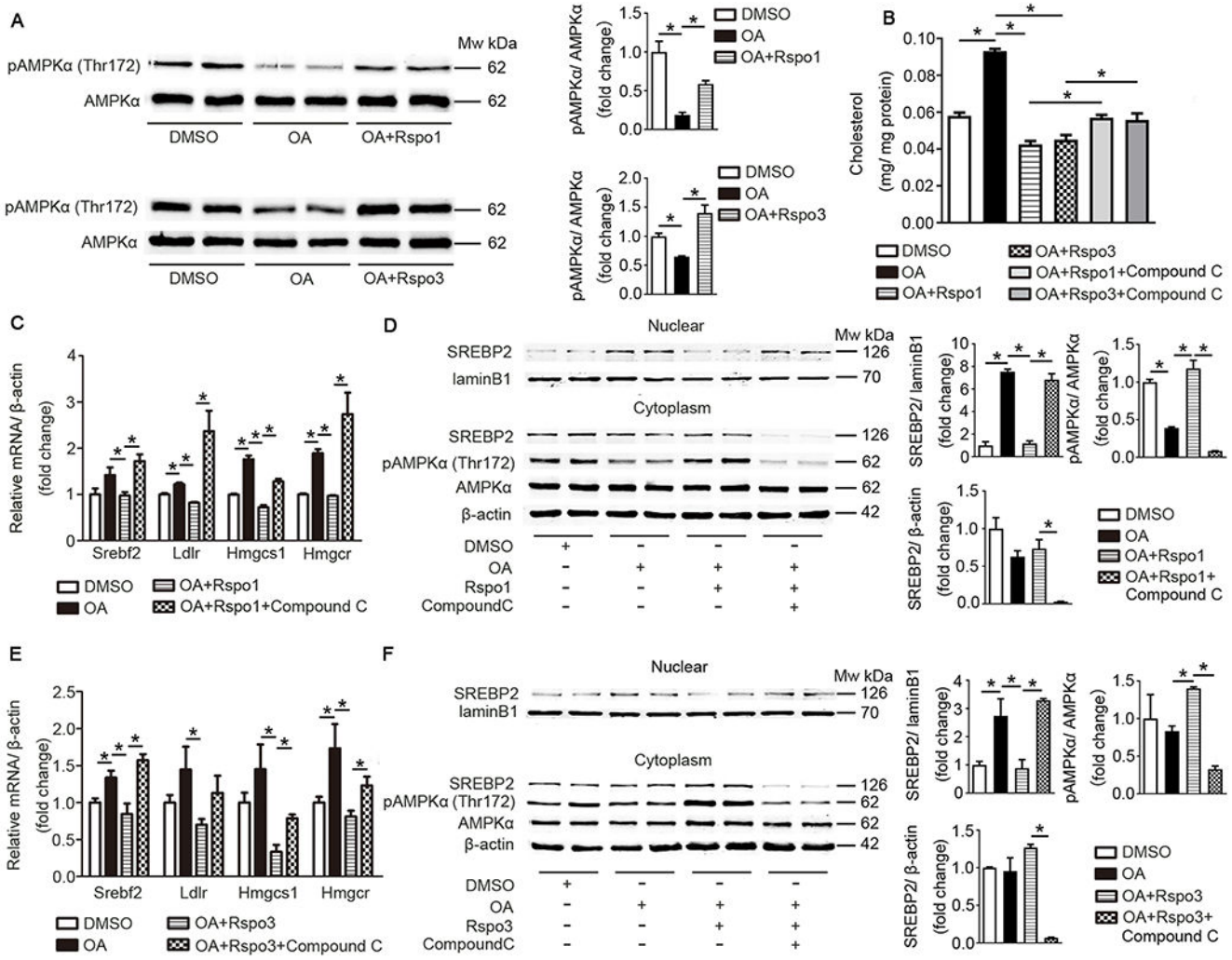

Figure 5. Rspo1/3 inhibits cholesterol synthesis through activating AMPKα.

A. Rspo1/3 promoted activation of AMPKα. AML12 cells were treated with OA for 24h, and then incubated with Rspo1/Rspo3 for 6h. Western blotting was performed to detect protein levels. The relative expression levels of proteins were calculated using Image J software. Shown is the representative of at least 3 repeat experiments.

B. Compound C diminished the inhibitory effects of Rspo1/3 on cholesterol accumulation. AML12 cells were treated with OA for 24h, followed by Rspo1/Rspo3 for 6h. Afterwards, AML12 cells were incubated with compound C (40μM) for 1h. Cholesterol contents in hepatocytes were then determined by assay kits. n=4.

C. Compound C diminishes the inhibitory effects of Rspo1 on cholesterol uptake and synthesis. After indicated treatments, mRNA was extracted from hepatocytes and analyzed by quantitive RT-PCR. n=6.

D. Compound C diminishes the inhibitory effects of Rspo1 on nuclear translocation of SREBP2. Western blotting was performed to detect protein levels. The relative expression levels of proteins were calculated using Image J software. Shown is the representative of at least 3 repeat experiments.

E. Compound C diminishes the inhibitory effects of Rspo3 on cholesterol uptake and synthesis. After indicated treatments, mRNA was extracted from hepatocytes and analyzed by quantitive RT-PCR. n=6.

F. Compound C diminishes the inhibitory effects of Rspo3 on nuclear translocation of SREBP2. Western blotting was performed to detect protein levels. The relative expression levels of proteins were calculated using Image J software. Shown is the representative of at least 3 repeat experiments.

Data are represented as mean±SEM. *p<0.05.

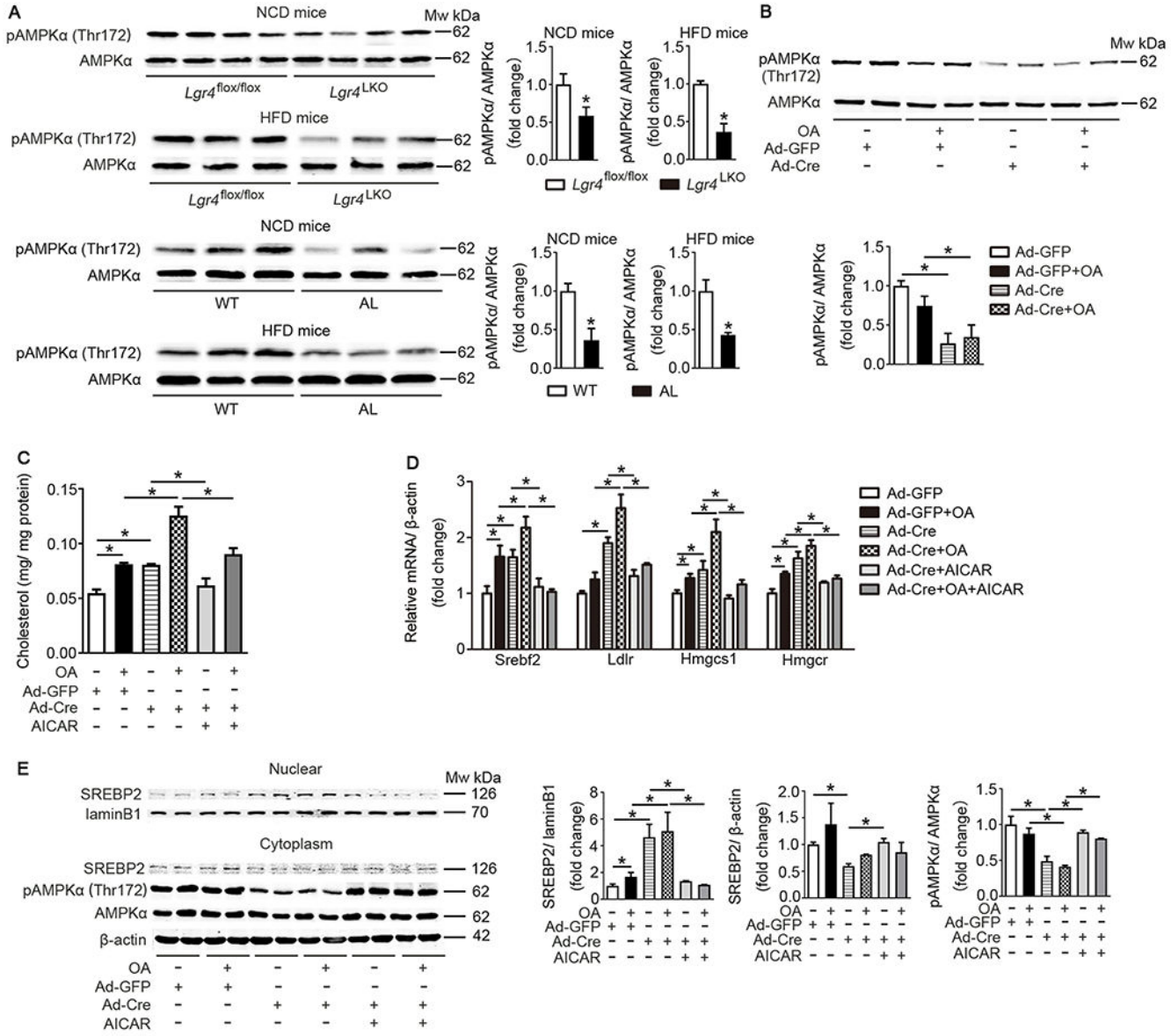

Figure 6. LGR4 ablation promotes cholesterol synthesis through inhibiting AMPKα.

A. Transient and stable hepatic LGR4 knockdown repressed AMPKα activation. Western blotting was performed to detect level of AMPKα phosphorylation in liver. The relative expression levels of proteins were calculated using Image J software. Shown is the representative of at least 3 repeat experiments.

B. LGR4 depletion suppressed AMPKα activation in hepatocytes. Western blotting was performed to detect level of AMPKα phosphorylation in *Lgr4*$^{flox/flox}$ primary hepatocytes after indicated treatment. The relative expression levels of proteins were calculated using Image J software. Shown is the representative of at least 3 repeat experiments.

C. AICAR reversed LGR4 knockdown-induced cholesterol accumulation. *Lgr4*$^{flox/flox}$ primary hepatocytes were incubated with Ad-Cre or Ad-GFP for 48h, followed by AICAR

(0.5mM) treatment for 1h. Cholesterol contents in hepatocytes of different treatments were then determined by assay kits. n=4.

D. AICAR reversed LGR4 knockdown-induced cholesterol uptake and synthesis. After indicated treatments, mRNA was extracted from hepatocytes and analyzed by quantitive RT-PCR.

E. AICAR reversed LGR4 knockdown-induced nuclear translocation of SREBP2. Western blotting was performed to detect protein levels. The relative expression levels of proteins were calculated using Image J software. Shown is the representative of at least 3 repeat experiments.

Data are represented as mean±SEM. *p<0.05.

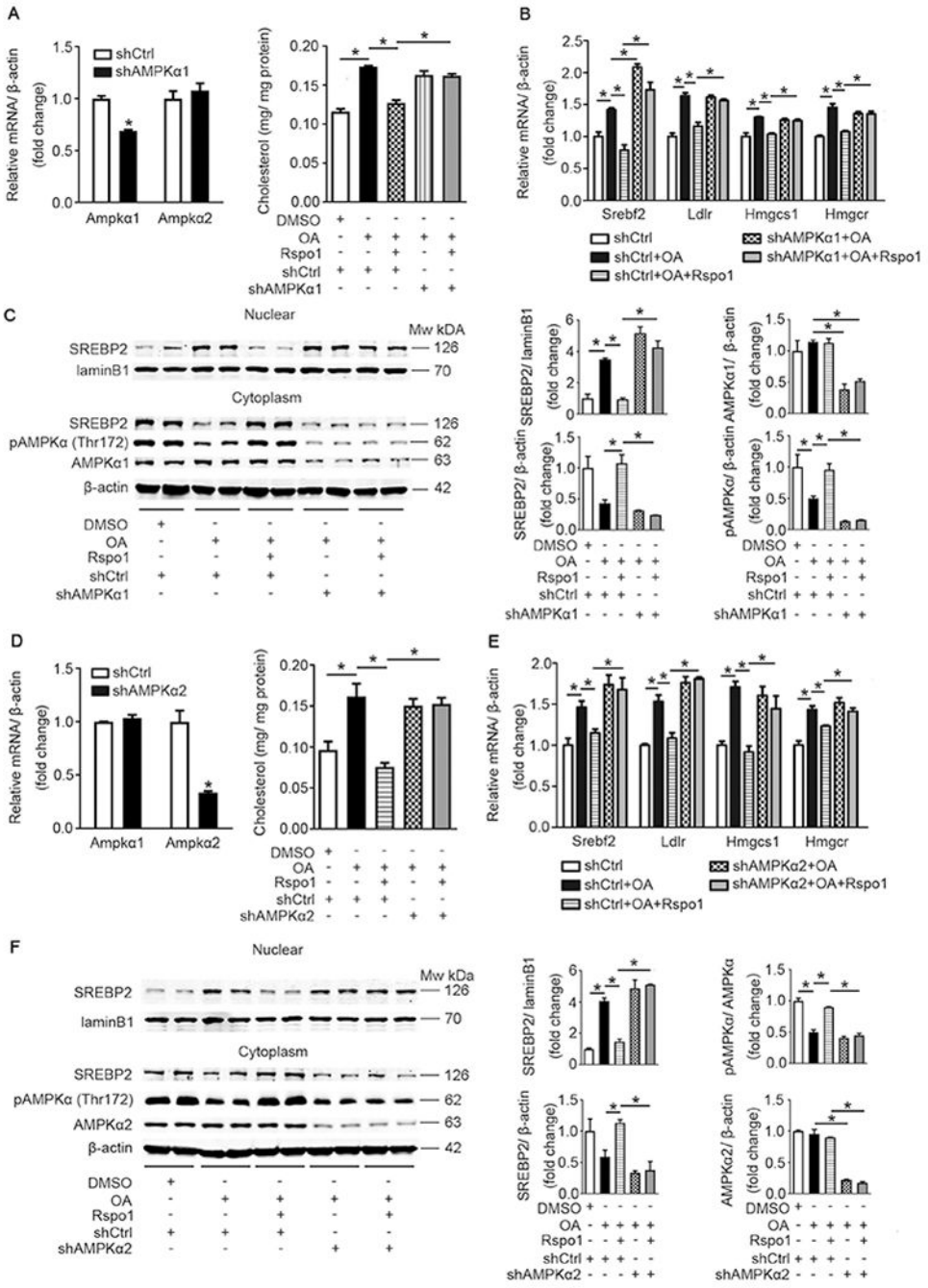

Figure 7. AMPKα1/2 knockdown abolished the inhibitory effects of Rspo1-LGR4 signaling on hepatic cholesterol synthesis.

A. AMPKα1 knockdown diminishes the inhibitory effects of Rspo1 on cholesterol accumulation. AML12 cells were transfected with AMPKα1 shRNA for 36h. mRNA were extracted from hepatocytes and analyzed by quantitive RT-PCR. n=6. *p<0.05 vs. shCtrl. After the transfection, cells were treated by OA for 24h and stimulated by Rspo1 for 6h. Cholesterol contents in hepatocytes after different treatments were determined by assay kits. n=4.

B. AMPKα1 knockdown reversed Rspo1 induced downregulation of genes related to cholesterol uptake and synthesis. After indicated treatments, mRNA was extracted from hepatocytes and analyzed by quantitive RT-PCR.

C. AMPKα1 knockdown diminishes the inhibitory effects of Rspo1 on nuclear translocation of SREBP2. Western blotting was performed to detect protein levels. The relative expression levels of proteins were calculated using Image J software. Shown is the representative of at least 3 repeat experiments.

D. AMPKα2 knockdown diminishes the inhibitory effects of Rspo1 on cholesterol accumulation. AML12 cells were transfected with AMPKα2 shRNA for 36h, mRNA were extracted from hepatocytes and analyzed by quantitive RT-PCR. n=6. *p<0.05 vs. shCtrl. After the transfection, cells were treated by OA for 24h and stimulated by Rspo1 for 6h. Cholesterol contents in hepatocytes after different treatments were determined by assay kits. n=4.

E. AMPKα2 knockdown reversed Rspo1 induced downregulation of genes related to cholesterol uptake and synthesis. After indicated treatments, mRNA was extracted from hepatocytes and analyzed by quantitive RT-PCR. n=6.

F. AMPKα2 knockdown diminishes the inhibitory effects of Rspo1 on nuclear translocation of SREBP2. Western blotting was performed to detect protein levels. The relative expression levels of proteins were calculated using Image J software. Shown is the representative of at least 3 repeat experiments.

Data are represented as mean±SEM. *p<0.05.

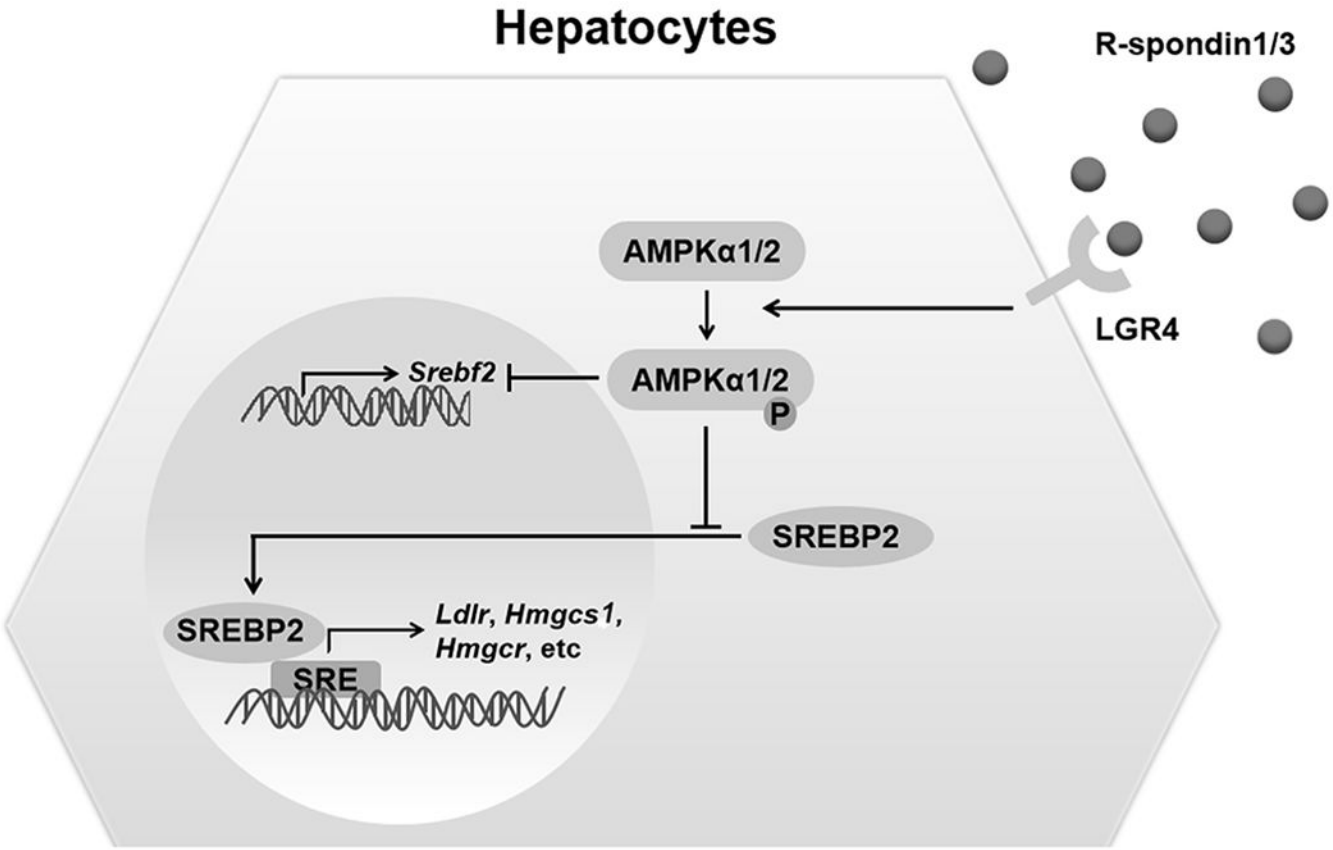

Figure 8. Schematic diagram showing the mechanism by which Rspo1/Rspo3-LGR4 signaling inhibits hepatic cholesterol synthesis.

In hepatocytes, Rspo1/3 bind to their receptor LGR4 to promote phosphorylate of AMPKα. The activated AMPKα will further restrain the expression and nuclear translocation of SREBP2, therefore, downregulate transcription of genes related to cholesterol uptake and synthesis, including *Ldlr*, *Hmgcs1* and *Hmgcr*.